湖州师范学院
Huzhou University

STAR 25 YEARS

Measurement of Light Nuclei Production in Au+Au Collisions at $\sqrt{s_{NN}} = 3 - 200$ GeV from RHIC-STAR

刘慧 (for the STAR Collaboration)

Huzhou University

April 26, 2025

第二十届全国中高能核物理大会暨第十四届全国中高能核物理专题研讨会，April 24-28, 2025，上海

Outline

- Introduction
- RHIC-STAR Experiment
- Results and Discussions
- Summary

Introduction - QCD Phase Transition

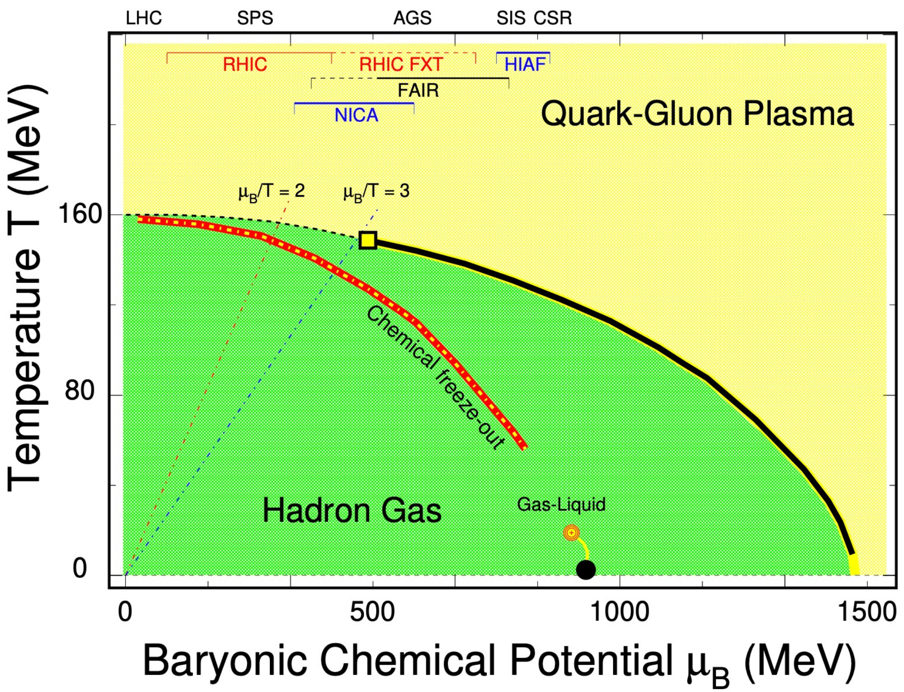

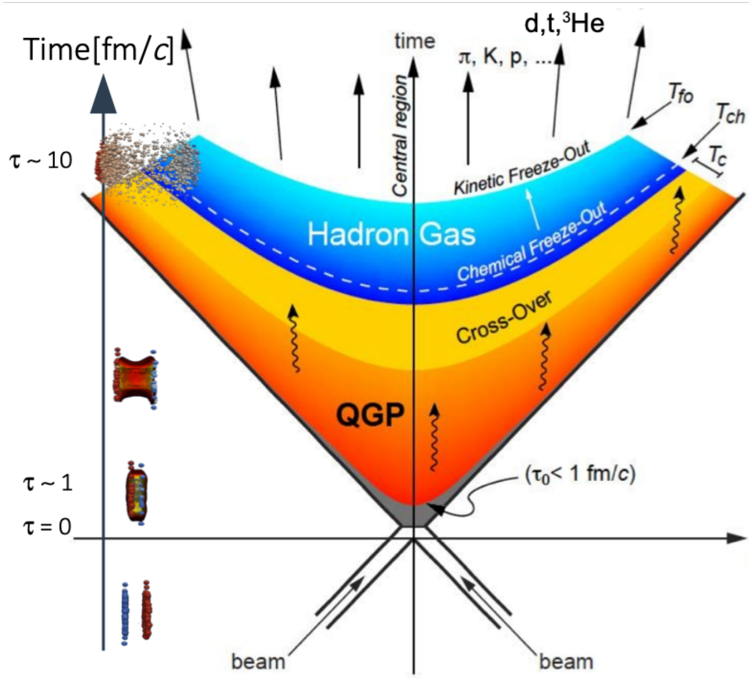

- **QCD Phase Transition**
  - High Temperature:
    QGP properties
  - High Baryon Density:
    Critical Point (CP) and 1st phase boundary
- **Chemical Freeze-Out**
  - Particle abundance is in equilibrium
- **Kinetic Freeze-Out**
  - The momentum distribution and kinetic energy of the particles are stabilized

Introduction - Light Nuclei

➢ Light Nuclei

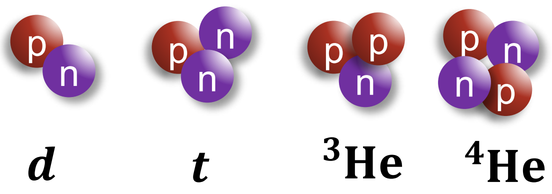

Loosely bound objects with small binding energies

➢ Light Nuclei Production Mechanism

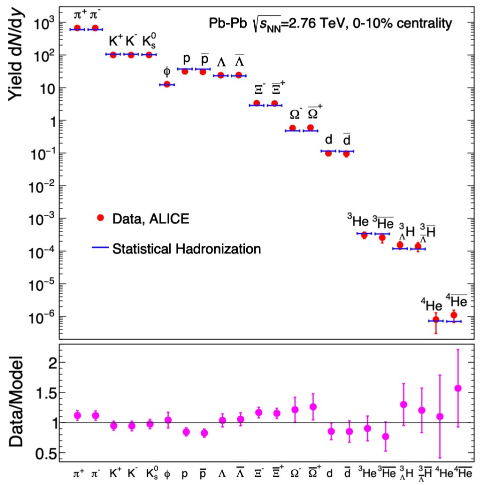

➢ Thermal approach

Light nuclei produced directly during the evolution of the system

The statistical-thermal model ($\boldsymbol{T_{ch}, \mu_B, V}$)

➢ Coalescence approach

Nucleons coalesce to form a composite particle after the kinetic freeze-out

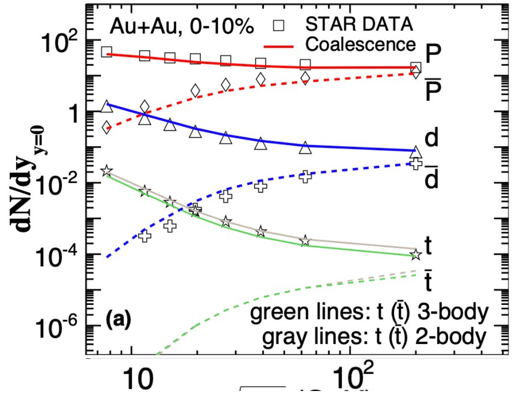

Transport + Wigner function ($\boldsymbol{p_i, r_i}$)
Transport + Coalescence model ($\boldsymbol{p_i, r_i, \Delta p, \Delta r}$)

A. Andronic et al, Phys.Lett.B 697 (2011) 203-207;
J. Cleymans et al, Phys.Rev.C 84 (2011) 054916;
A. Andronic et al, Nature 561 (2018) 7723, 321-330

K.J. Sun et al, Phys.Lett.B 792 (2019) 132-137;
W.B. Zhao et al, Phys.Rev.C 102 (2020) 4, 044912;
H. Liu et al, Phys.Lett.B 805 (2020) 135452;

Introduction - Compound Yield Ratio

➢ Compound Yield Ratio Sensitive Observations for Searching Critical Point and 1st order boundary

$$\frac{N_t \times N_p}{N_d^2} = \frac{N(\text{pnn})\times N(\text{p})}{N(\text{pn})\times N(\text{pn})} \approx \frac{1}{2\sqrt{3}}\left[1 + \boxed{\Delta n} + \frac{\lambda}{\sigma}\boxed{G\left(\frac{\xi}{\sigma}\right)}\right]$$

- λ: varies smoothly with T and μ_B of emission source
- $\sigma \approx r_d \approx r_t$ is the root-mean-radius of light nuclei

➢ Neutron Density Fluctuation (Δn)

In the case of a first-order phase transition in which two phases coexist, the system could have large density inhomogeneity and therefore large density fluctuations

➢ Long-range Correlation ($G(\frac{\xi}{\sigma})$)

Near the critical point, the correlation length (ξ) of the system increases, and the nucleus become long-range correlations.

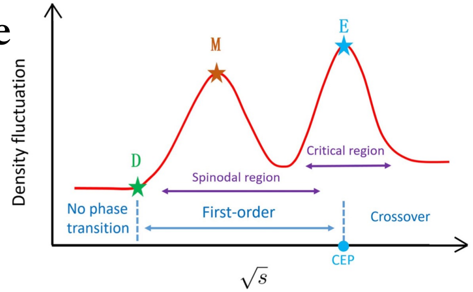

K.J. Sun et al, Phys.Lett.B 781 (2018) 499-504;
K.J. Sun et al, Phys.Lett.B 816 (2021) 136258

[STAR Collaboration] Phys.Rev.Lett. 130 (2023) 202301

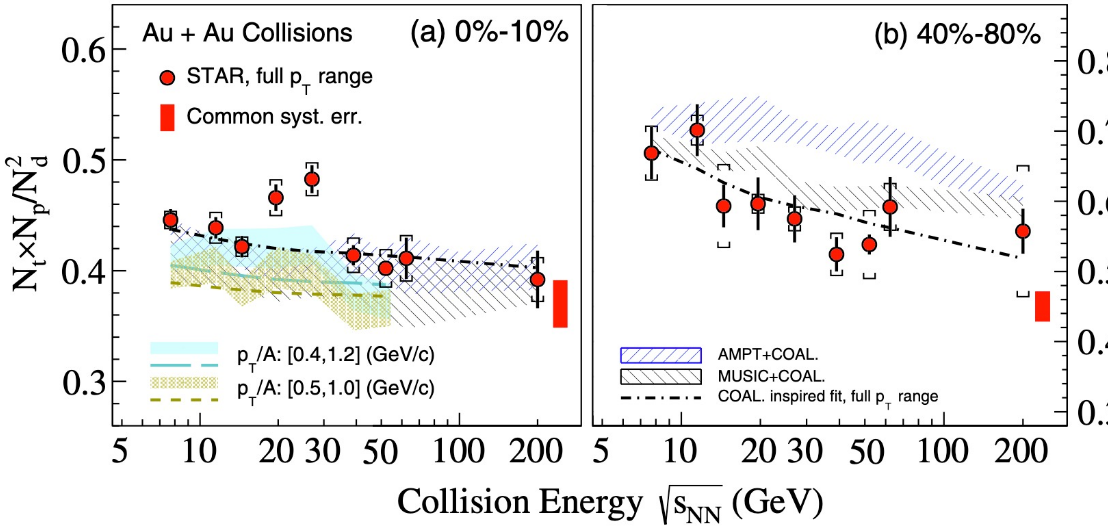

➢ Non-monotonic behavior of yield ratio vs. energy observed from 0-10% central Au+Au collisions of STAR experiment, possibly signaling a critical point and/or 1st order phase transition

STAR Detector

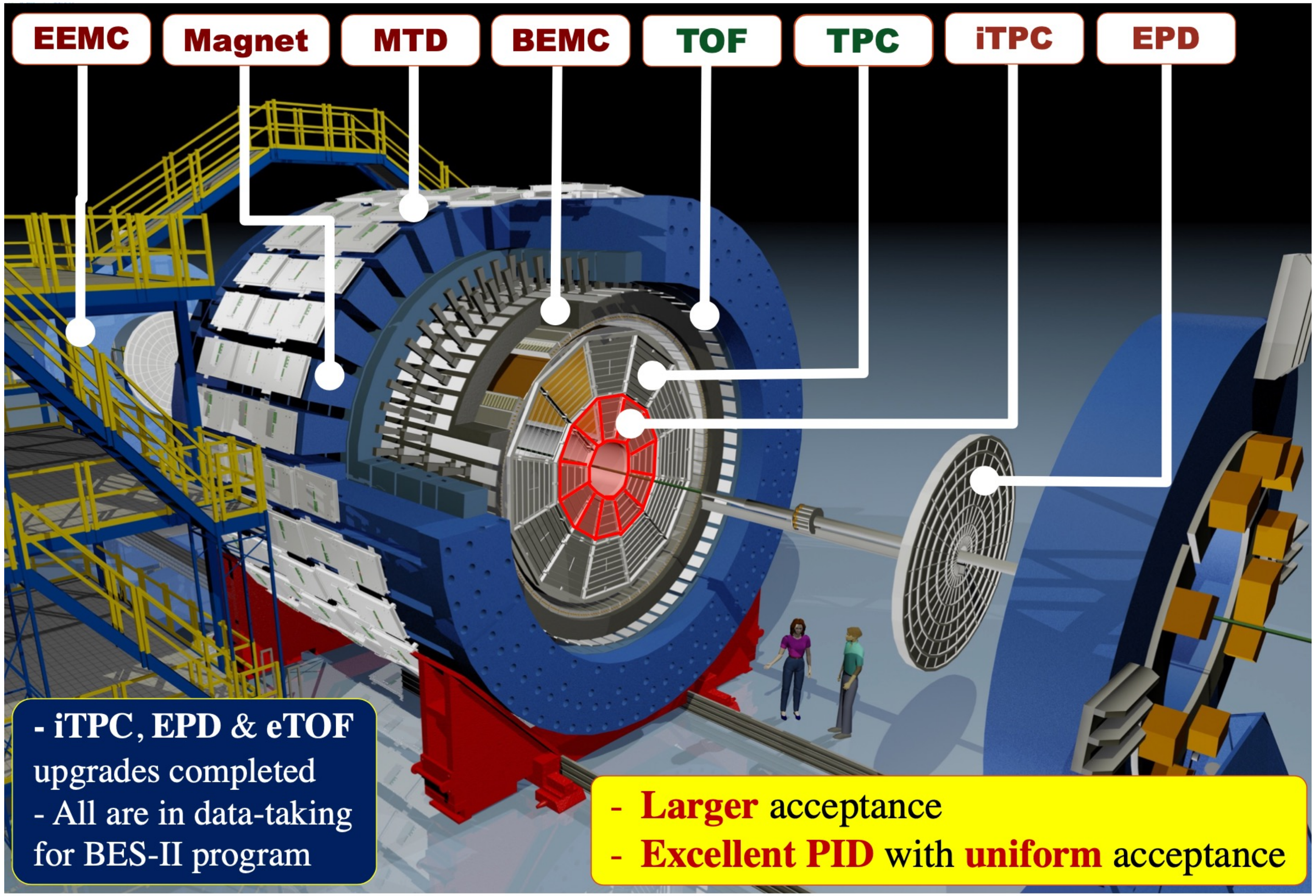

Main sub-detectors for PID

- ➢ Time Projection Chamber (TPC)
  - Ionization energy loss (dE/dx)
- ➢ Time of Flight (TOF)
  - $m^2 = p^2(c^2t^2/L^2 - 1)$

BES-II Upgrades

- ➢ iTPC (2019+)
  - Extended η acceptance and improved tracking and dE/dx resolution
- ➢ eTOF (2019+)
  - Extended PID coverage
- ➢ EPD (2018+)
  - Improved EP resolution

Beam Energy Scan Program

Data collected by STAR Au+Au collisions

- BES I : 2010 – 2017, Collider mode
- BES II: 2018 – Now, Collider / FXT mode

Au+Au collisions at RHIC (BES I)			
$\sqrt{s_{NN}}$ (GeV)	nEvents (M)	μ_B (MeV)	T_{ch} (MeV)
200	236	25	166
62.4	47	73	165
54.4	566	83	165
39	89	112	164
27	32	156	162
19.6	16	206	160
14.5	13	264	156
11.5	7	320	152
7.7	3	420	140

Au+Au BES II	$\sqrt{s_{NN}}$ (GeV)	E_{beam} (GeV)	nEvents (M)	μ_B (MeV)
Collider mode	27	---	356	156
	19.6	---	478	206
	17.3	---	256	230
	14.6	---	324	262
Collider mode / Fixed-Target mode	13.7	100	51	280
	11.5	70 / ---	52 / 235	320
	9.2	44.5 / ---	54 / 162	370
	7.7	31.2 / ---	113 / 101	420
Fixed-Target mode	7.2	26.5	89	440
	6.2	19.5	118	490
	5.2	13.5	103	540
	4.5	9.8	108	590
	3.9	7.3	117	633
	3.5	5.75	116	670
	3.2	4.59	201	699
	3.0	3.85	260 / 2103	750

Particle Signal Extraction

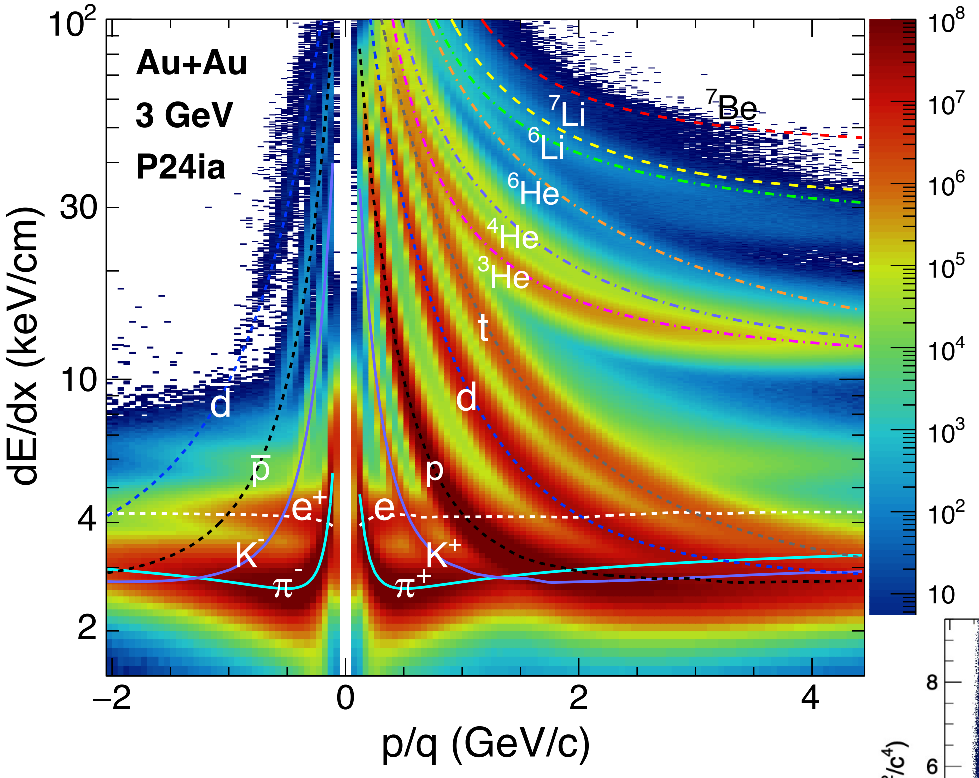

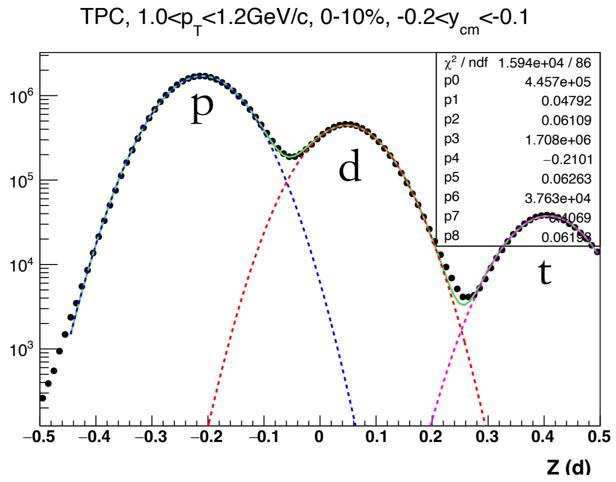

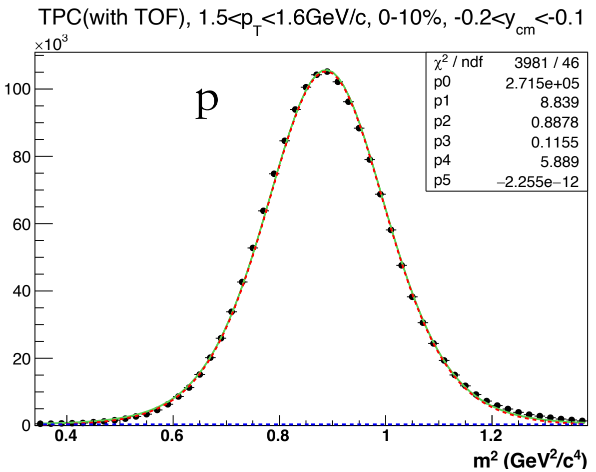

$$Z = ln\frac{\langle dE/dx\rangle}{\langle dE/dx\rangle_{Bichsel}}$$

$$m^2 = p^2\left(\frac{c^2t^2}{L^2} - 1\right) = p^2(\frac{1}{\beta^2} - 1)$$

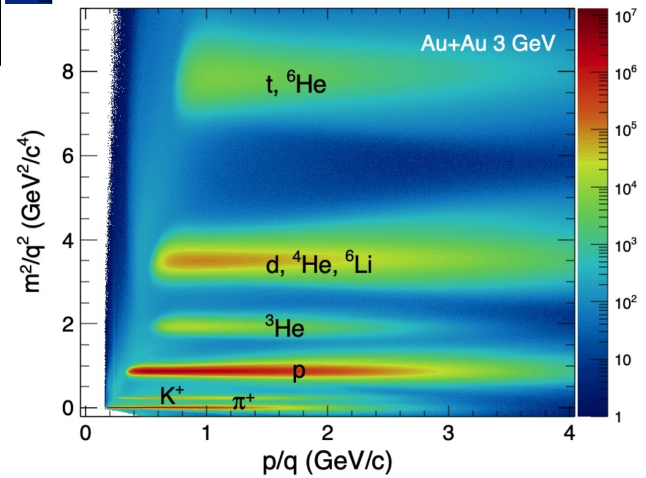

- Gaussian function fit (low p_T)

$$f(x) = p_0 \times exp[-\frac{1}{2}(\frac{x-p_1}{p_2})^2]$$

- Student-t function (high p_T)

$$f(T|p_1) = \frac{\Gamma(\frac{p_1+1}{2})}{\sqrt{p_1\pi}\Gamma(\frac{p_1}{2})}(1+\frac{T^2}{p_1})^{-\frac{p_1+1}{2}}$$

$$T = \frac{x-p_2}{p_3}, \Gamma(z) = \int_0^{\infty} t^{z-1}e^{-t}dt$$

Transverse Momentum Spectra

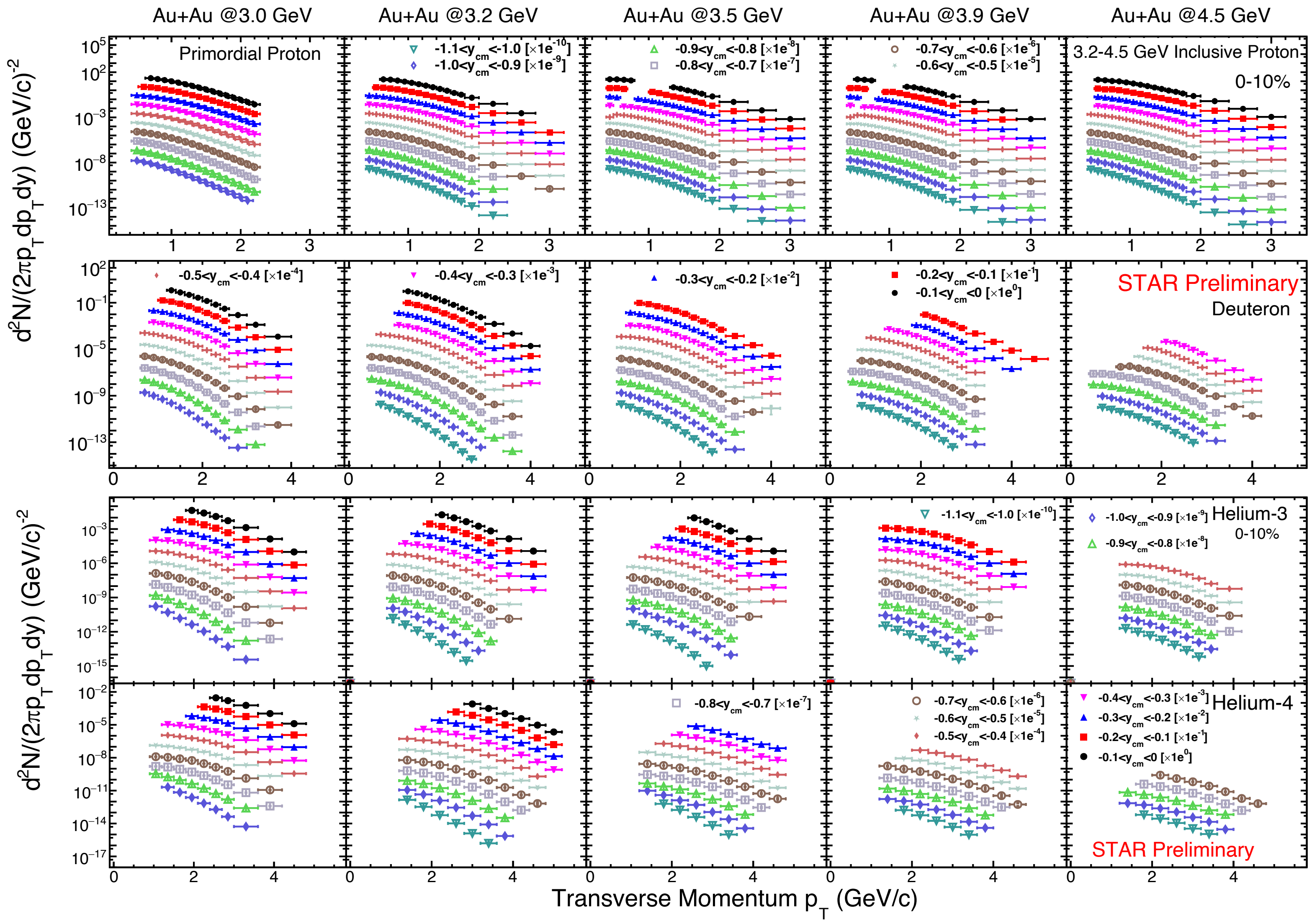

QM2025, Liubing Chen (CCNU)

- Transverse momentum spectra of ***p***, ***d***, **^{3}He**, and **^{4}He** as a function of rapidity in Au+Au collisions at $\sqrt{s_{NN}}$ = 3.0 - 4.5 GeV with FXT mode
- Good coverage from target rapidity to middle rapidity for collision energies

Transverse Momentum Spectra

QM2025, Yixuan Jin (CCNU)

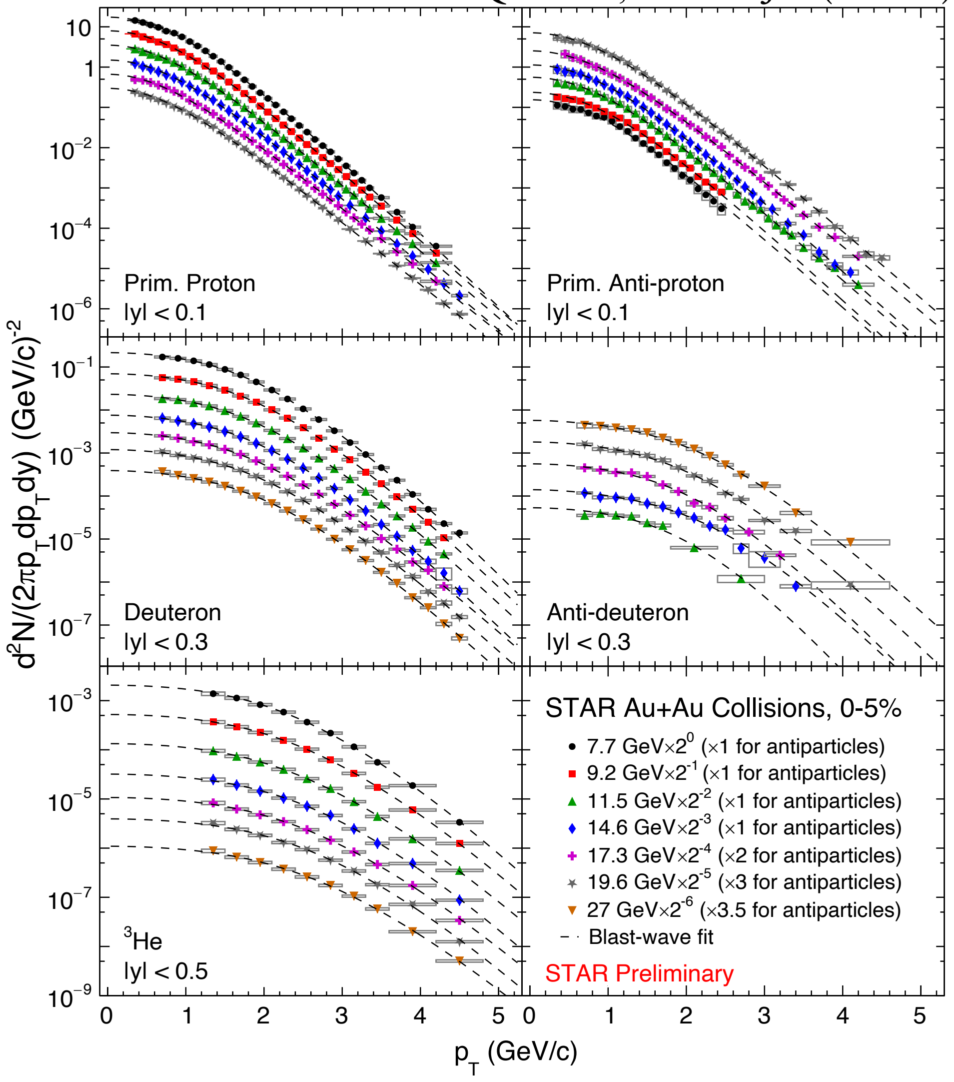

- Transverse momentum spectra of $\boldsymbol{p}$, $\boldsymbol{\bar{p}}$, $\boldsymbol{d}$, $\boldsymbol{\bar{d}}$, and ^{3}**He** at mid-rapidity in Au+Au collisions at $\sqrt{s_{NN}}$ = 7.7 - 27 GeV with BES-II collider mode
- The low $\boldsymbol{p_T}$ reach is extended in BES-II, which leads to smaller systematic uncertainties in $\boldsymbol{p_T}$-integrated yields

- Blast-Wave Function

$$\frac{1}{2\pi p_T}\frac{d^2N}{dp_T dy} \propto \int_0^R r dr m_T I_0\left(\frac{p_T \sinh\rho}{T_{kin}}\right) K_1\left(\frac{m_T \cosh\rho}{T_{kin}}\right)$$

$$\rho = \tanh^{-1}\beta_r,\ \beta_r(r) = \beta_T\left(\frac{r}{R}\right)^n$$

Kinetic Freeze-out Parameters:

T_{kin} : kinetic freeze-out temperature
$\langle\beta_T\rangle$: average radial flow velocity

n : n=1 (I_0 and K_1 are from Bjorken Hydrodynamic assumption)

J.D. Bjorken, Phys.Rev.D 27 (1983) 140-151;
E. Schnedermann et al. Phys.Rev.C 48 (1993) 2462-2475

Averaged Transverse Momentum $\langle p_T \rangle$

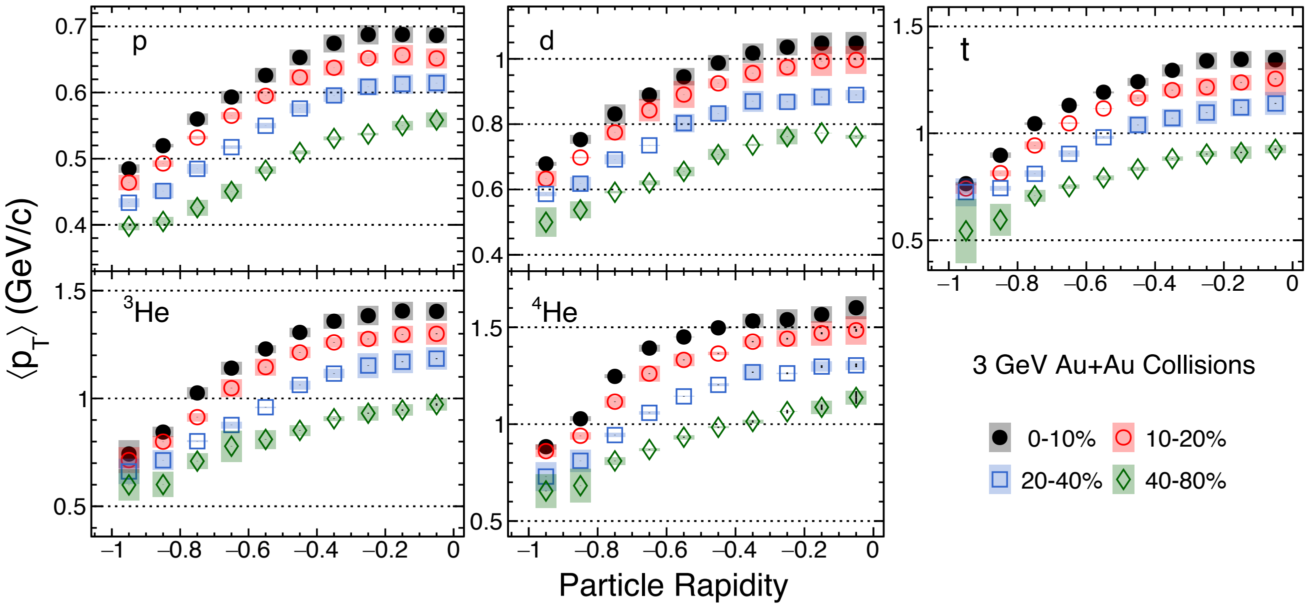

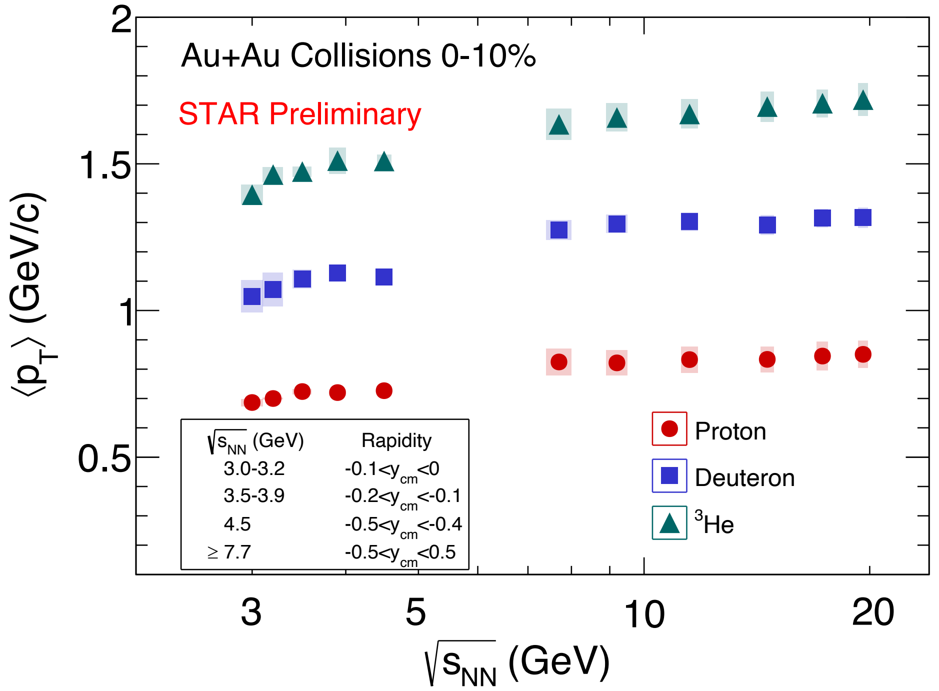

- $\langle p_T \rangle$ of protons and light nuclei as a function of centrality, rapidity, and collision energy
- Centrality dependence reflects that the collective expansion in the radial direction is stronger in central collisions than in peripheral collisions
- Hint of $\langle p_T \rangle$ increase with energy for 4.5 GeV and below, flat trend between 7.7 and 19.6 GeV. This behavior will be studied in 4.5 - 7.7 GeV in the future

[STAR Collaboration] Phys. Rev. C 110 (2024) 054911

Integrated Yields dN/dy

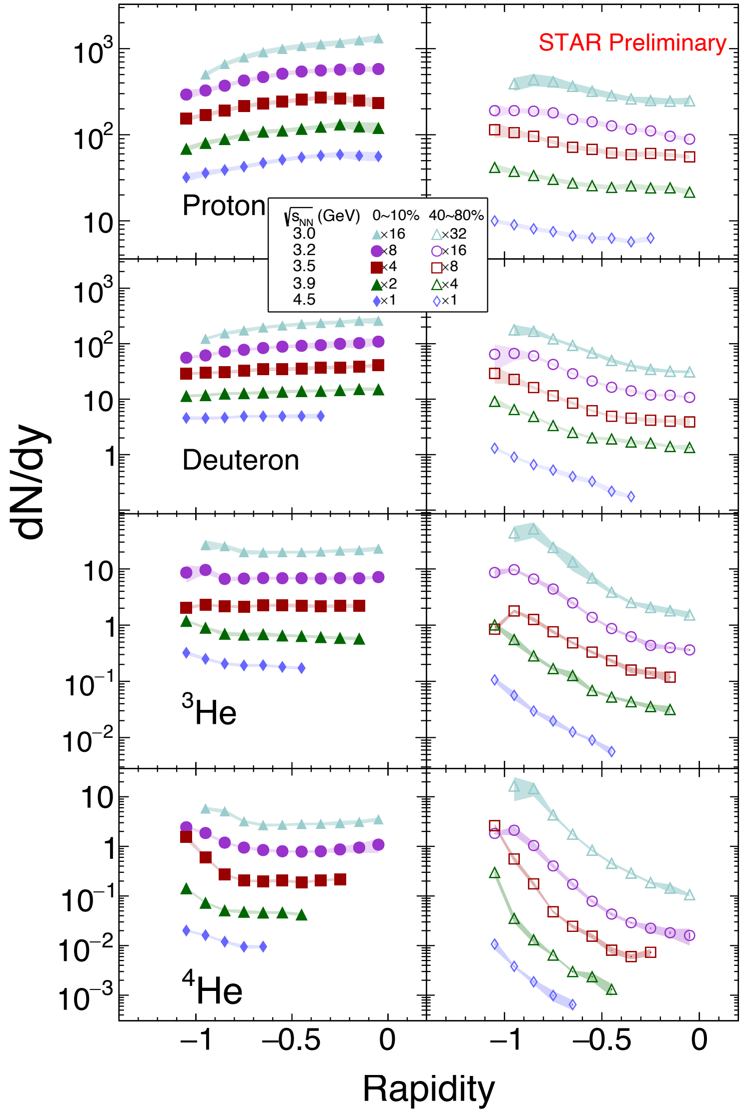

QM2025, Liubing Chen

- dN/dy of protons and light nuclei show significant centrality and rapidity dependence at 3 – 4.5 GeV
- The particle which has large nuclear number will has more sensitive dN/dy distribution from target to middle rapidity, and from central collisions to peripheral collisions. It implies that fragments have impact on the production of light nuclei
- The band indicate systematical uncertainty

Particle Mass Dependence of dN/dy

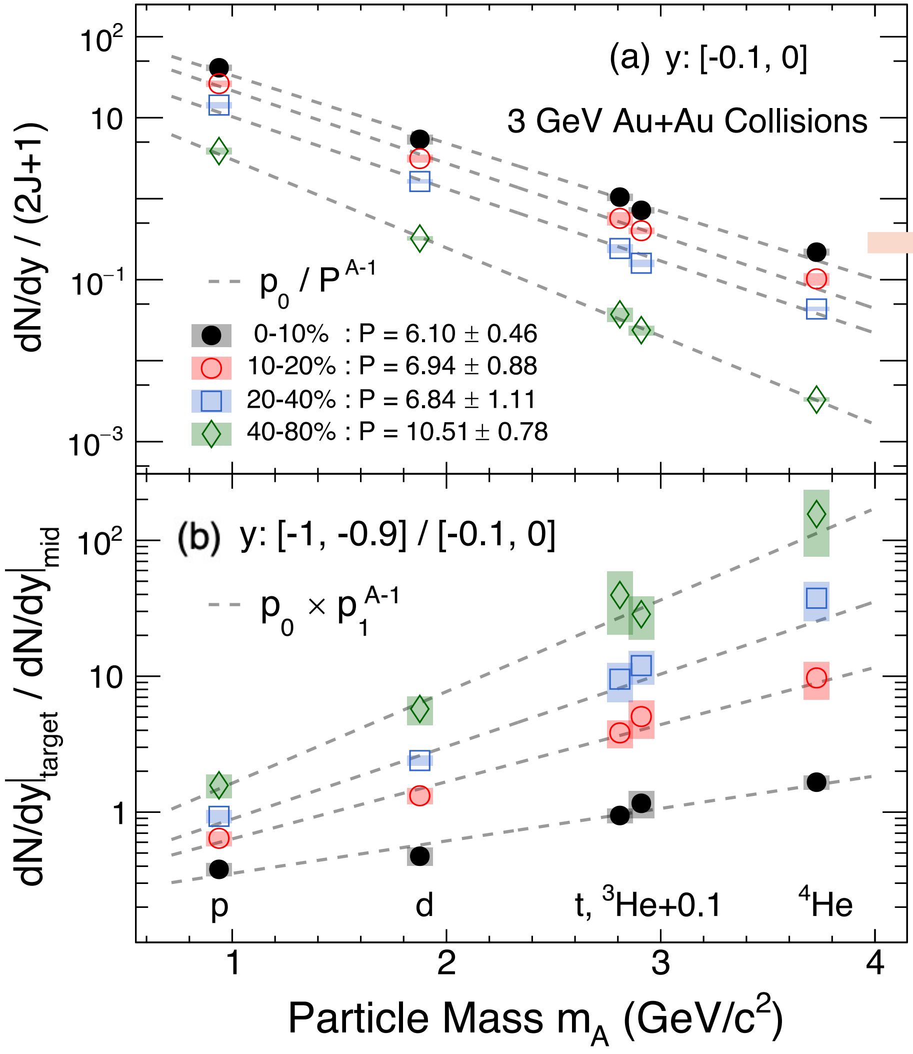

- Cluster production yields change drastically with the atomic mass number A

$$f(m_A) = p_0/P^{A-1}$$

$$P = e^{\frac{m-\mu_B}{T}}$$

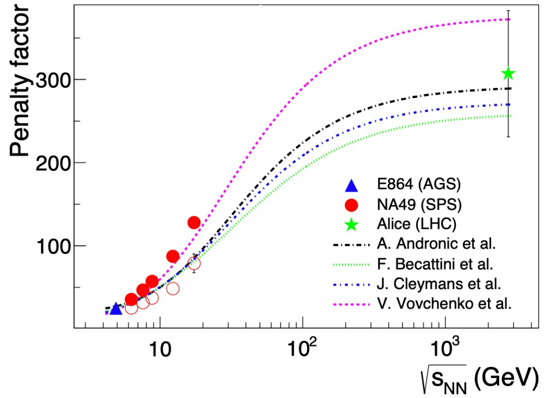

- The penalty factor (P) increases from the central to peripheral collisions, implying that light nuclei are more likely to form in central collisions

- The target to mid-rapidity ratio indicates that as the light nuclei become heavier, the proportion of contributions originating from the nuclear fragments increases

[NA49 Collaboration] Phys. Rev. C 94, 044906 (2016)
[E864 Collaboration] Phys. Rev. Lett. 83, 5431 (1999)

Energy Dependence of dN/dy

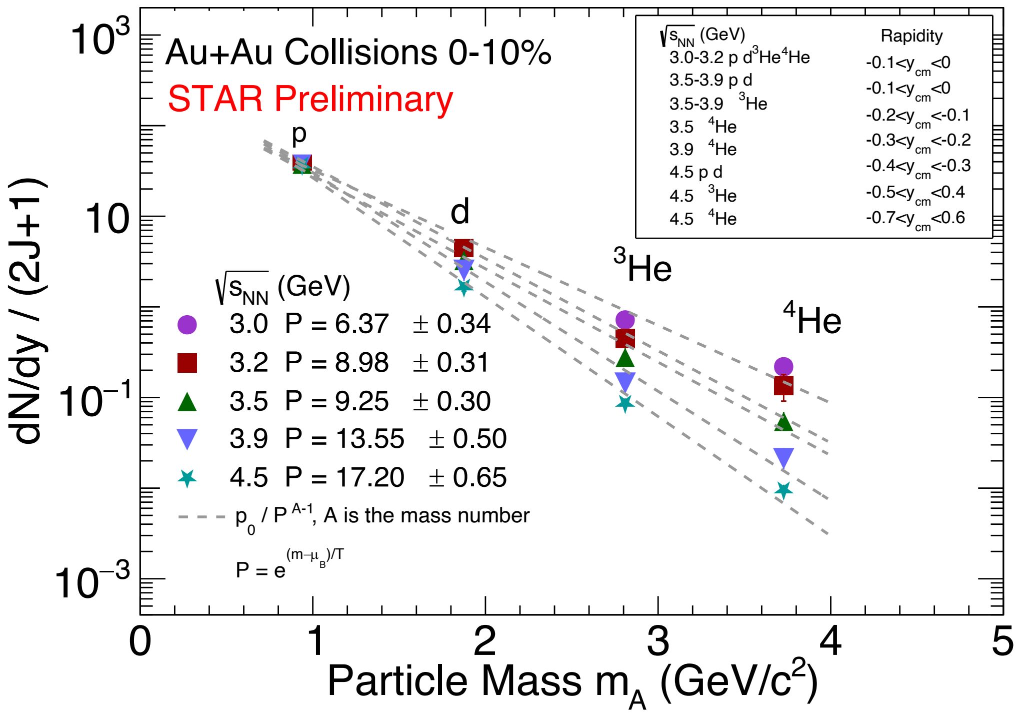

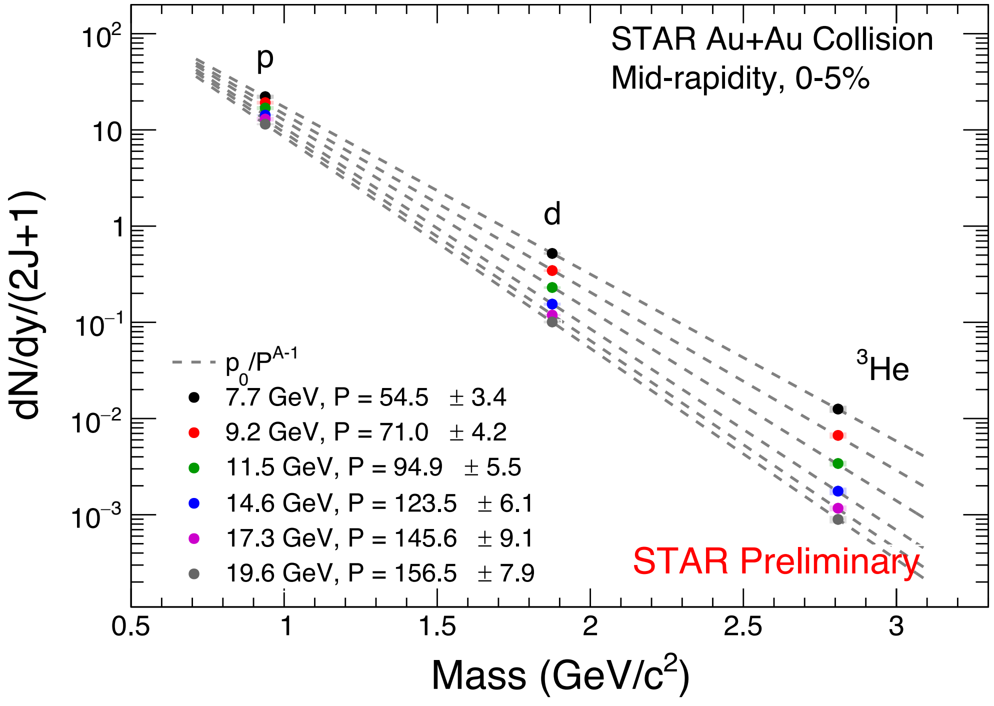

- The production of light nuclei are proportional to the spin degeneracy
- Light nuclei yields decrease exponentially with increasing particle mass
- Slope decrease indicates that light nuclei are more easily formed at low energies

Particle Yield Ratios

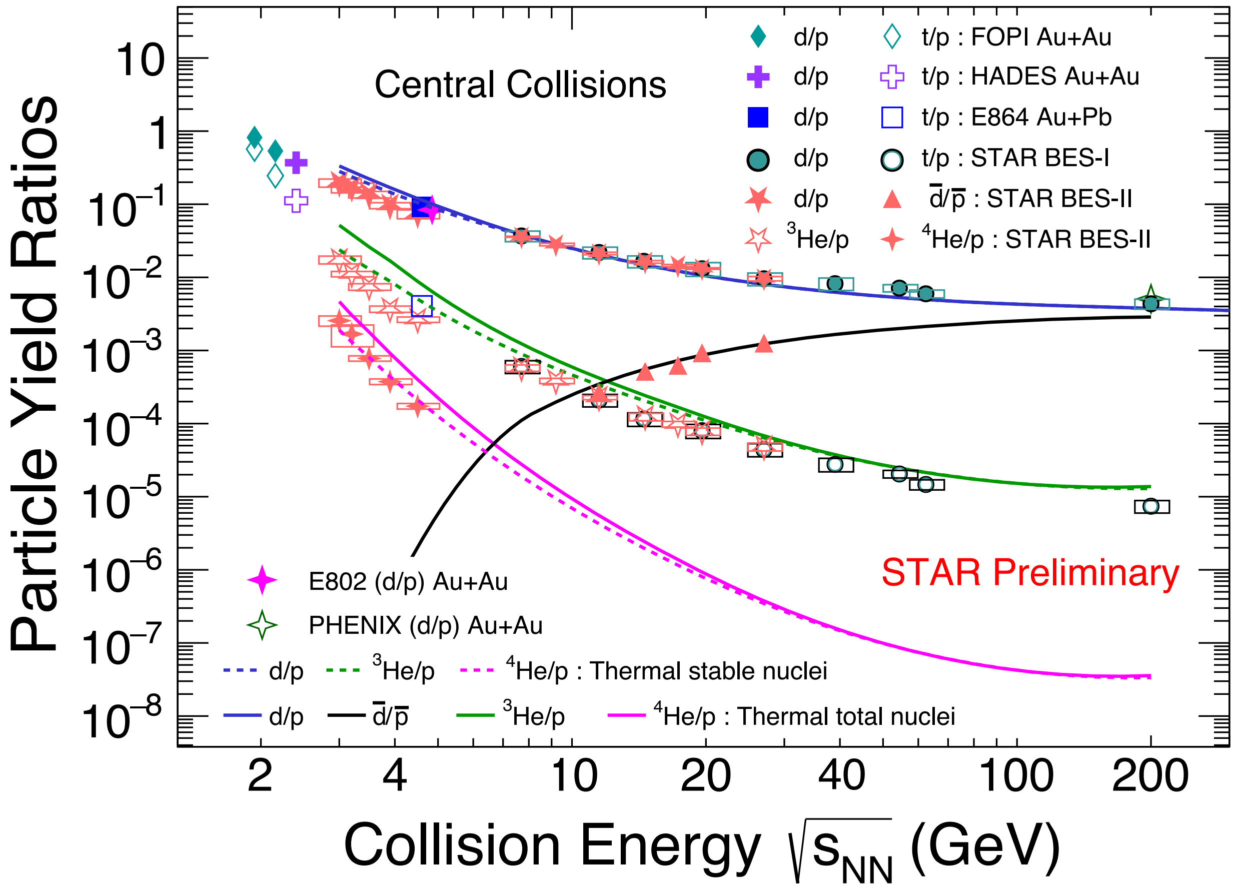

- Clear energy dependence is observed for both d/p, $\bar{d}/\bar{p}$, t/p, $^3\mathrm{He}/p$, and $^4\mathrm{He}/p$ ratios
- The trends of ratios can be described qualitatively by the thermal model
- t/p and $^3\mathrm{He}/p$ were overestimated by thermal model, possibly due to the hadronic re-scattering effect
- Considering only stable nuclei, $^4\mathrm{He}/p$ from thermal model is consistent with the experiment data

K. Sun et al. Nature Commun. 15 (2024) 1, 1074
[STAR Collaboration] Phys. Rev. C 96, 044904 (2017); Phys.Rev.Lett. 130 (2023) 202301;
[E802 Collaboration] Phys.Rev.C 60 (1999) 064901;[E864 Collaboration] Phys.Rev.C 61 (2000) 064908;
[FOPI Collaboration] Nucl.Phys.A 848 (2010) 366-427;V. Vovchenko, et al. Phys. Rev. C 93(2016) 6, 064906;

Coalescence Parameters

$$E_A \frac{d^3N_A}{dp_A^3} = B_A\left(E_p \frac{d^3N_p}{dp_p^3}\right)^Z \left(E_n \frac{d^3N_n}{dp_n^3}\right)^{A-Z} \approx (n/p)^{A-Z} B_A\left(E_p \frac{d^3N_p}{dp_p^3}\right)^A \Big|_{p_p=p_n=\frac{p_A}{A}}$$

QM2025, Yixuan Jin

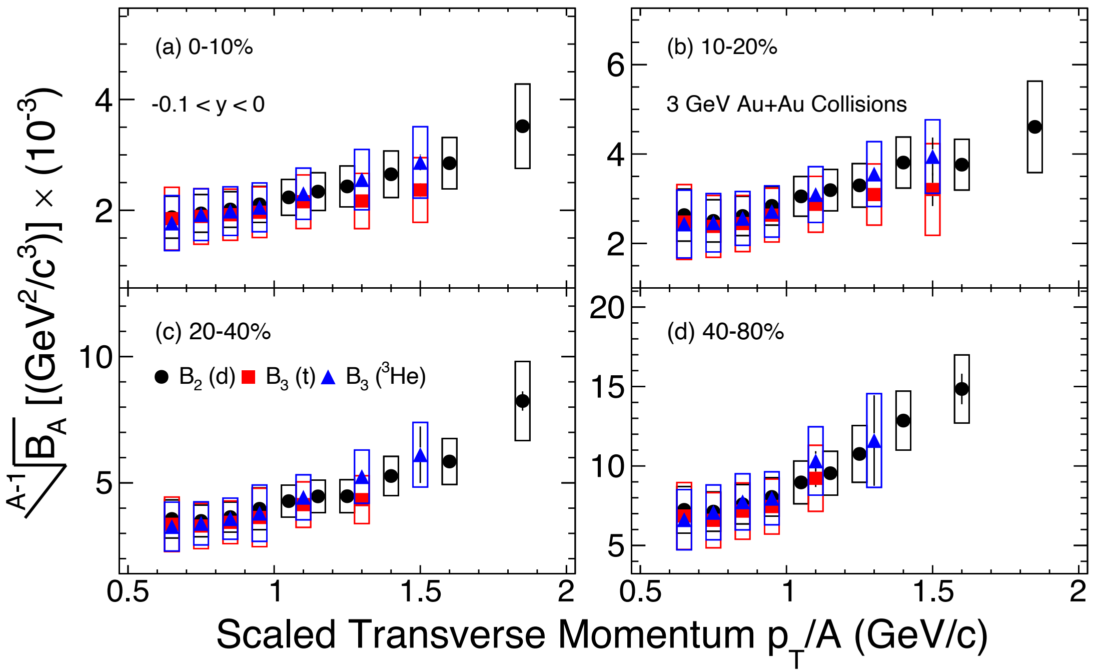

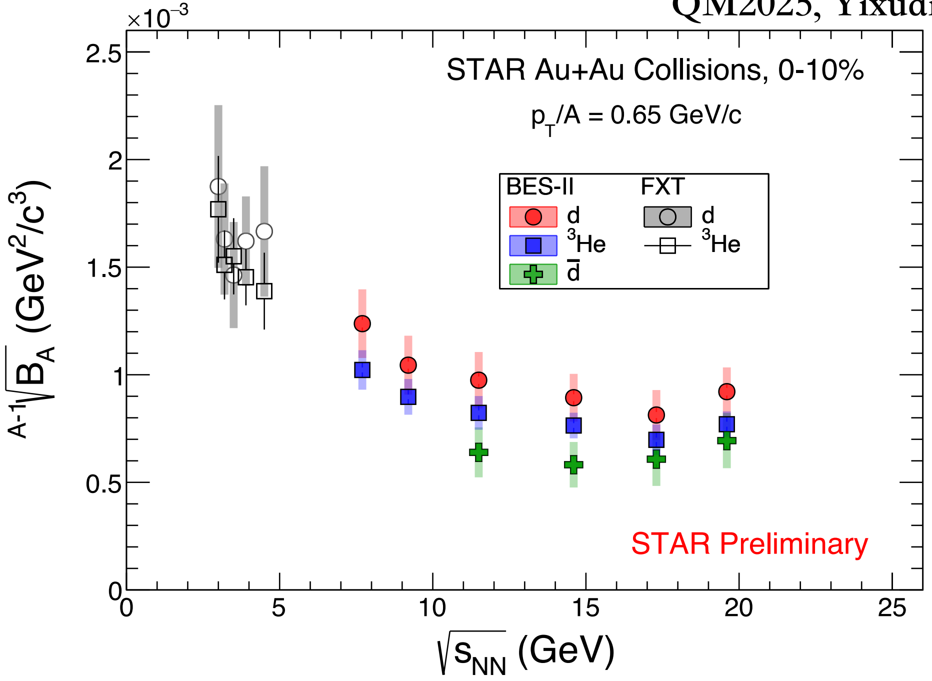

- $B_A \propto (1/V_{eff})^{(A-1)}$ reflects the region of homogeneity and the freeze-out property
- Length of homogeneity becomes smaller in peripheral collisions and at higher p_T region
- $\sqrt[A-1]{B_A}$ decrease with increasing energy, which indicates the effective volume V_{eff} increases with increasing energy

R. Scheibl and U. Heinz Phys.Rev.C 59 (1999) 1585-1602; S. Zhang et al. Phys.Lett.B 684 (2010) 224-227

Compound Yield Ratios

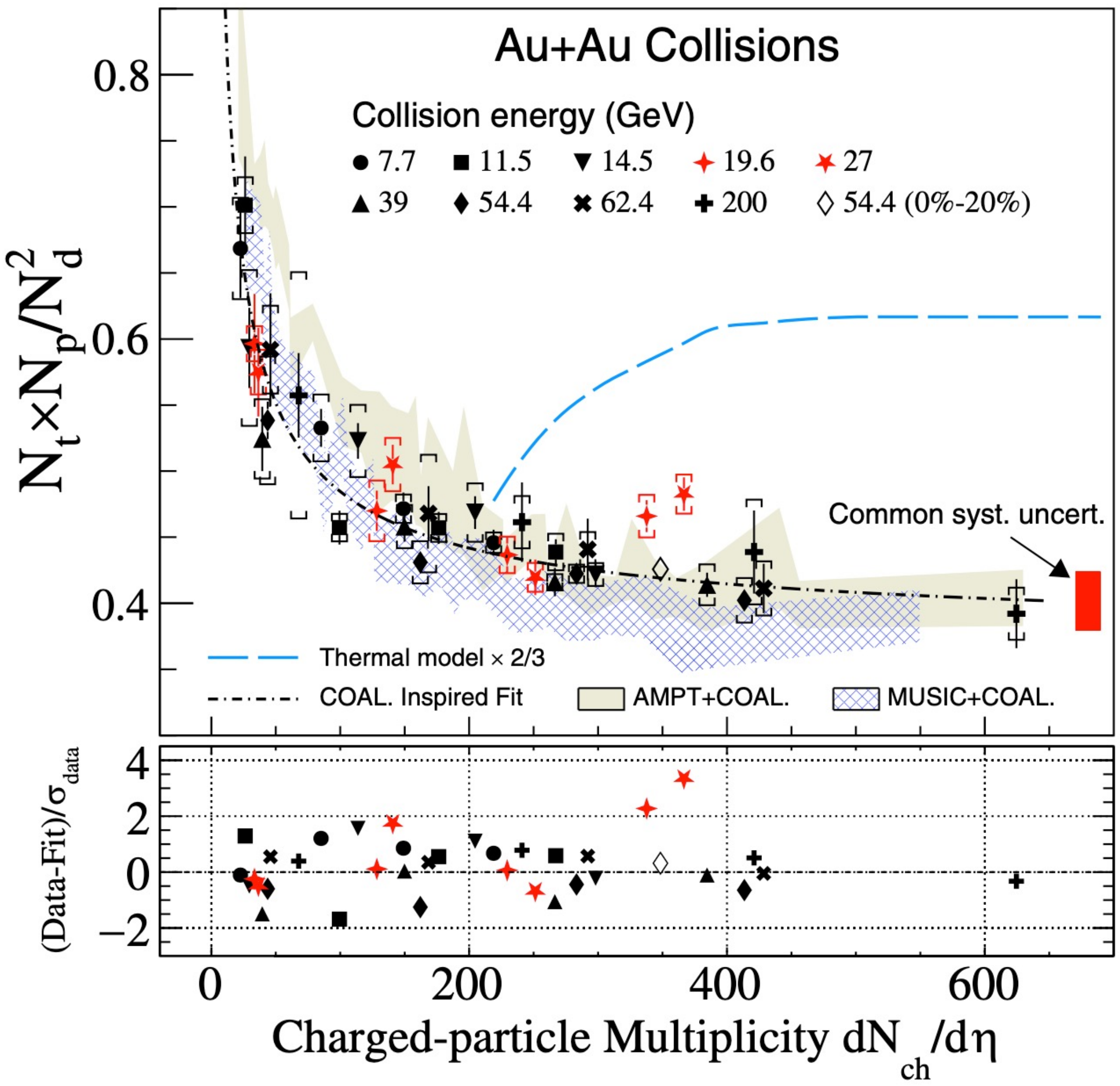

- The yield ratio $N_t \times N_p / N_d^2$ as a function of charged-particle multiplicity $dN_{ch}/d\eta$ ($|\eta| < 0.5$)
- It is observed that the yield ratio $N_t \times N_p / N_d^2$ exhibits scaling, regardless of collision energy and centrality

Coal. inspired fit: $\frac{N_t \times N_p}{N_d^2} \propto \left(\frac{R^2 + \frac{2}{3} r_d^2}{R^2 + \frac{1}{2} r_t^2}\right)^3$

$R \propto (dN_{ch}/d\eta)^{1/3}, r_d = 1.96\ fm, r_t = 1.59\ fm$

- An enhancement with a significance of 4.1σ is observed at 19.6 and 27 GeV, while no enhancement is observed at 54.4 GeV for the same $dN_{ch}/d\eta$ value

BES-II analysis with high statistics is in progress

[STAR Collaboration] Phys.Rev.Lett. 130 (2023) 202301

Energy Dependence of Compound Yield Ratios

in progress

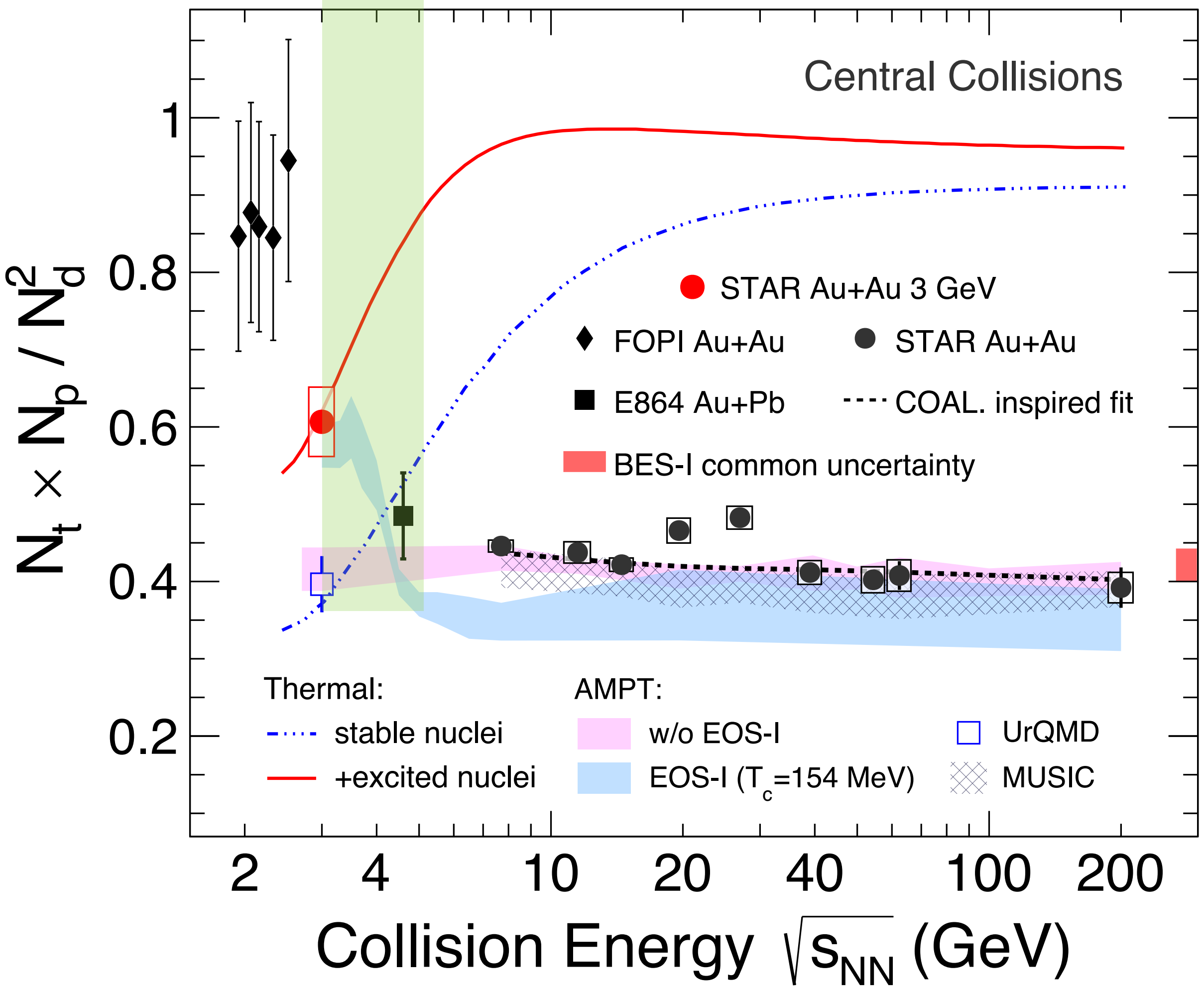

- The yield ratio $N_t{\times}N_p/N_d^2$ at mid-rapidity in 3 GeV 0-10% Au+Au collisions follow the world trend of the energy dependence and monotonically increase with decreasing energies
- The thermal model shows the energy-dependent trend contrary to experiments
- The yield ratio can be reproduced by the AMPT model when employing a first-order phase transition by input the critical temperature of 154 MeV

V. Vovchenko, et al. Phys. Rev. C 93(2016) 6, 064906
E. Shuryak et al. Eur.Phys.J.A 56 (2020) 9, 241
K. Sun et al. Phys.Rev.C 103 (2021) 6, 064909
K. Sun et al. arXiv: 2205.11010

Compound Yield Ratios at 3 GeV

$$\frac{N_t \times N_p}{N_d^2} = \frac{N(\text{pnn}) \times N(\text{p})}{N(\text{pn}) \times N(\text{pn})} \approx \frac{1}{2\sqrt{3}}\left[1 + \Delta n + \frac{\lambda}{\sigma} G\left(\frac{\xi}{\sigma}\right)\right]$$

$$\frac{N_{^4\text{He}} \times N_p}{N_{^3\text{He}} \times N_d} = \frac{N(\text{ppnn}) \times N(\text{p})}{N(\text{ppn}) \times N(\text{pn})} \approx \frac{2\sqrt{2}}{9\sqrt{3}}\left[1 + C_{np} + \Delta p + \frac{2\lambda}{\sigma} G\left(\frac{\xi}{\sigma}\right)\right]$$

C_{np} is the correlation between n and p density fluctuation

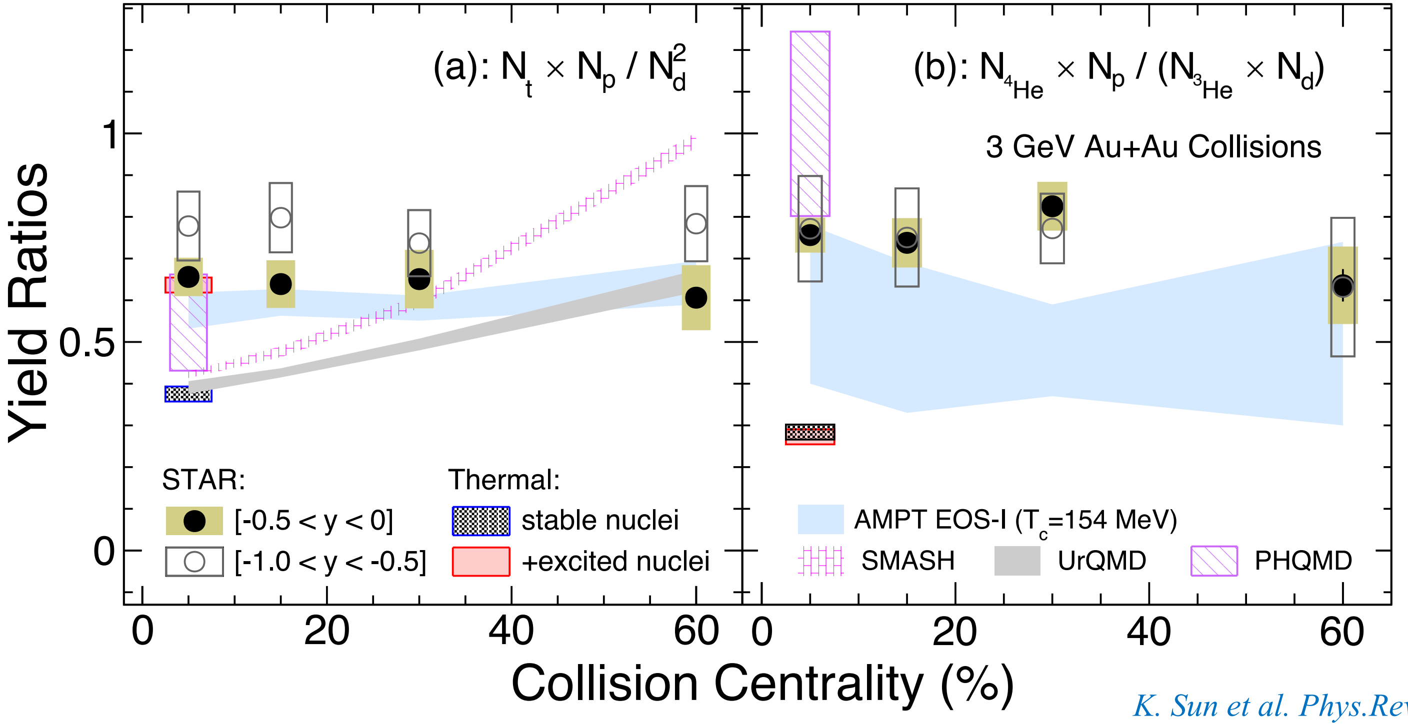

- The yield ratio $N_t \times N_p / N_d^2$
  - The AMPT model calculations with a first-order phase transition can describe the rapidity trend
  - The thermal model with excited nuclei contributions can describe the data
- The yield ratio $N_{^4\text{He}} \times N_p / (N_{^3\text{He}} \times N_d)$
  - No obvious rapidity and centrality dependence
  - No model describes the experimental results well

Ratio including ^{3}He and ^{4}He is in progress

K. Sun et al. Phys.Rev.C 103 (2021) 6, 064909; E. Shuryak et al. Eur.Phys.J.A 56 (2020) 9, 241

Kinetic Freeze-out Dynamics

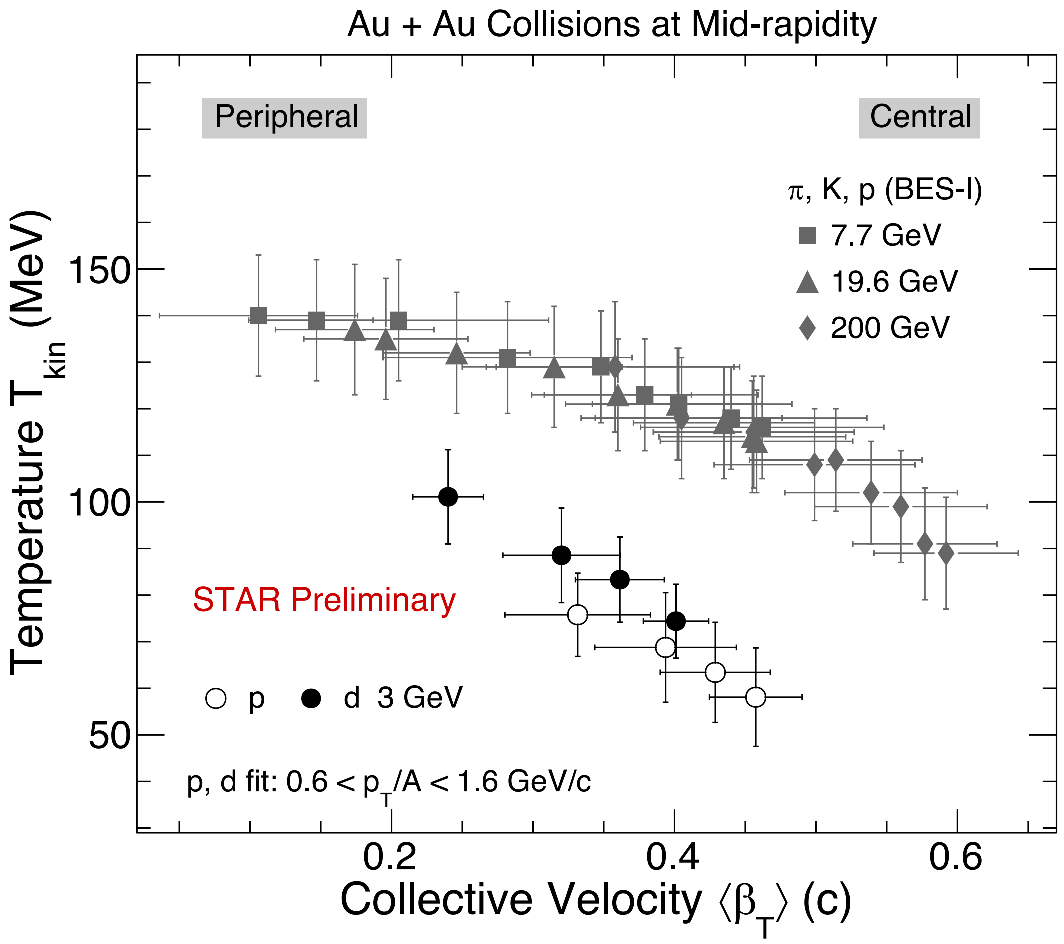

- T_{kin} versus $\langle \beta_T \rangle$ show a clear gap region between 3 GeV and energies above 7.7 GeV

Kinetic Freeze-out Dynamics

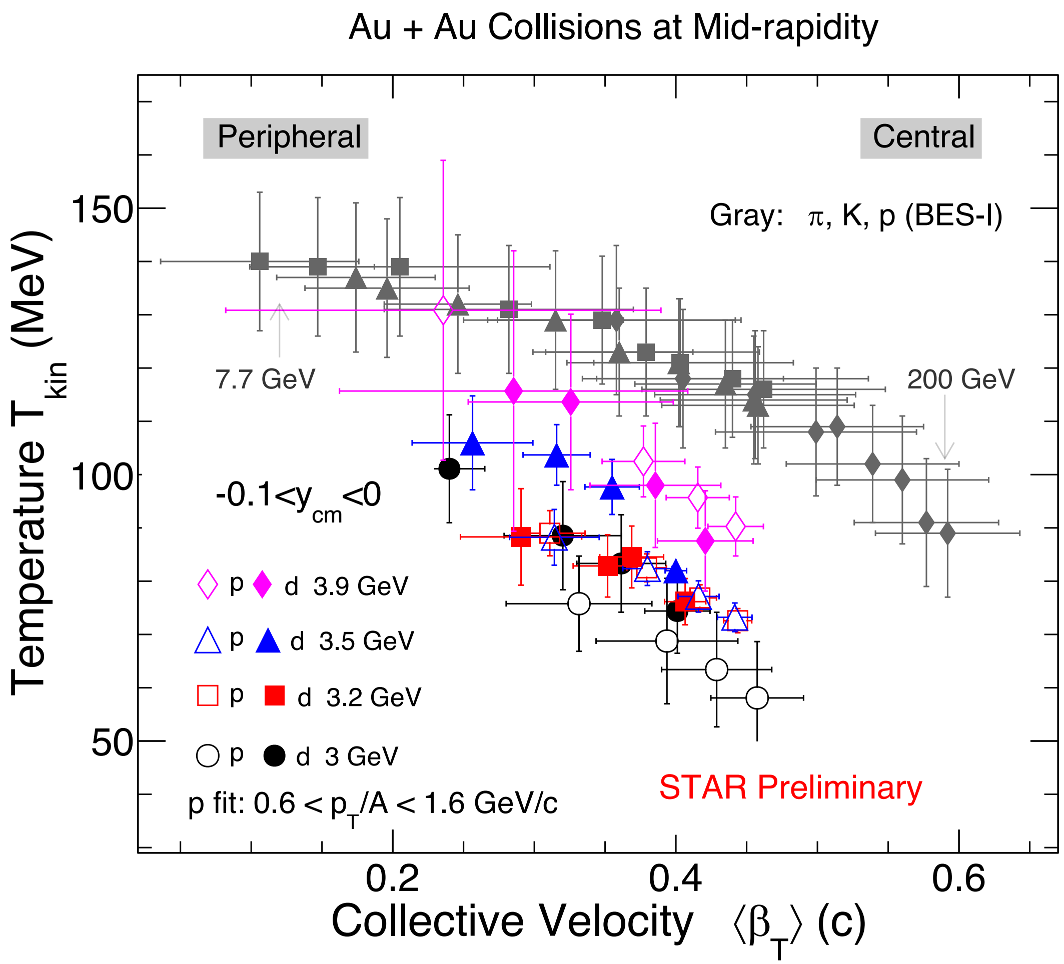

- $\mathrm{T_{kin}}$ versus $\langle\beta_T\rangle$ distribution shows a clear gap region between 3 GeV and energies above 7.7 GeV
- The gap can be filled by collision energies $\sqrt{s_{NN}}$ = 3.0 - 3.9 GeV, may imply a different medium equation of state (EoS)
- The differing trends in $\mathrm{T_{kin}}$ and $\langle\beta_T\rangle$ for protons and deuterons ($\sqrt{s_{NN}}$ = 3.0-3.9 GeV) imply they have distinct kinetic freeze-out surfaces

Summary

- We present light nuclei production (p_T spectra, dN/dy, $\langle p_T \rangle$, particle ratio, and B_A) and kinetic freeze-out parameters (T_{kin}, $\langle \beta_T \rangle$) in Au+Au collisions at $\sqrt{s_{NN}}$ = 3.0 - 4.5 GeV by STAR experiment, studying their rapidity and energy dependence
- We present p, d, ^{3}He, $\bar{p}$ and $\bar{d}$ production in Au+Au collisions at $\sqrt{s_{NN}} = 7.7 - 27$ GeV from RHIC STAR BES-II
  - ➜ Particle ratios and compound yield ratios follow the world trend of the energy dependence
  - ➜ Provide constraints for experimental and theoretical studies of light nucleus formation mechanisms
- Blast-wave fits and kinetic freeze-out dynamic at $\sqrt{s_{NN}}$ = 3.0 – 3.9 GeV
  - ➜ T_{kin} vs. $\langle \beta_T \rangle$ shows a different trend indicated that EoS of the hot and dense medium below the 7.7 GeV collisions seems different from that of high energy collisions

- ☐ Extend measurements to heavier nuclei over a broad energy range from $\sqrt{s_{NN}}$ =3.0 - 27 GeV
- ☐ Systematic analysis of light nuclei yields and spectra to deep understanding on light nuclei production mechanisms

Summary

- We present light nuclei production (p_T spectra, dN/dy, $\langle p_T \rangle$, particle ratio, and B_A) and kinetic freeze-out parameters (T_{kin}, $\langle \beta_T \rangle$) in Au+Au collisions at $\sqrt{s_{NN}}$ = 3.0 - 4.5 GeV by STAR experiment, studying their rapidity and energy dependence
- We present p, d, ^{3}He, $\bar{p}$ and $\bar{d}$ production in Au+Au collisions at $\sqrt{s_{NN}} = 7.7 - 27$ GeV from RHIC STAR BES-II
  - ➜ Particle ratios and compound yield ratios follow the world trend of the energy dependence
  - ➜ Provide constraints for experimental and theoretical studies of light nucleus formation mechanisms
- Blast-wave fits and kinetic freeze-out dynamic at $\sqrt{s_{NN}}$ = 3.0 – 3.9 GeV
  - ➜ T_{kin} vs. $\langle \beta_T \rangle$ shows a different trend indicated that EoS of the hot and dense medium below the 7.7 GeV collisions seems different from that of high energy collisions

- ☐ Extend measurements to heavier nuclei over a broad energy range from $\sqrt{s_{NN}}$ =3.0 - 27 GeV
- ☐ Systematic analysis of light nuclei yields and spectra to deep understanding on light nuclei production mechanisms

Thank you

Backup Slides

Winger functions

In the coalescence model [22–25], the number of a light nucleus of mass number A and consisting of Z protons and N neutrons ($A = Z + N$) is given by the overlap of its Wigner function f_A with the phase-space distributions $f_p(\mathbf{x}_i, \mathbf{p}_i, t)$ of protons and $f_n(\mathbf{x}_j, \mathbf{p}_j, t)$ of neutrons [24,25],

$$\frac{dN_A}{d^3\mathbf{P}_A} = g_A \int \Pi_{i=1}^{Z} \boxed{p_i^\mu d^3\sigma_{i\mu} \frac{d^3\mathbf{p}_i}{E_i} f_{p/\bar{p}}(\mathbf{x}_i, \mathbf{p}_i, t_i)}$$
$$\times \int \Pi_{j=1}^{N} \boxed{p_j^\mu d^3\sigma_{j\mu} \frac{d^3\mathbf{p}_j}{E_j} f_{n/\bar{n}}(\mathbf{x}_j, \mathbf{p}_j, t_j)}$$
$$\times \underline{f_A(\mathbf{x}_1', ..., \mathbf{x}_Z', \mathbf{x}_1', ..., \mathbf{x}_N'; \mathbf{p}_1', ..., \mathbf{p}_Z', \mathbf{p}_1', ..., \mathbf{p}_N'; t')}$$
$$\times \delta^{(3)}\left(\mathbf{P}_A - \sum_{i=1}^{Z}\mathbf{p}_i - \sum_{j=1}^{N}\mathbf{p}_j\right),$$

number of (anti)p

number of (anti)n

$f_{p,n}(x, p, t)$ is obtained in the positions, momenta and times of protons and neutrons at their last scatterings

For deuteron and triton

masses. For the deuteron, its Wigner function is then

$$f_2(\boldsymbol{\rho}, \mathbf{p}_\rho) = 8\exp\left[-\frac{\boldsymbol{\rho}^2}{\sigma_d^2} - \mathbf{p}_\rho^2\sigma_d^2\right], \tag{2}$$

with the relative coordinate $\boldsymbol{\rho}$ and the relative momentum $\mathbf{p}_\rho$ defined as

$$\boldsymbol{\rho} = \frac{1}{\sqrt{2}}(\mathbf{x}_1' - \mathbf{x}_2'), \quad \mathbf{p}_\rho = \frac{1}{\sqrt{2}}(\mathbf{p}_1' - \mathbf{p}_2'). \tag{3}$$

For the triton, its Wigner function is

$$f_3(\boldsymbol{\rho}, \boldsymbol{\lambda}, \mathbf{p}_\rho, \mathbf{p}_\lambda)$$
$$= 8^2\exp\left[-\frac{\boldsymbol{\rho}^2}{\sigma_t^2} - \frac{\boldsymbol{\lambda}^2}{\sigma_t^2} - \mathbf{p}_\rho^2\sigma_t^2 - \mathbf{p}_\lambda^2\sigma_t^2\right], \tag{4}$$

with the additional relative coordinate $\boldsymbol{\lambda}$ and relative momentum $\mathbf{p}_\lambda$ defined as

$$\boldsymbol{\lambda} = \frac{1}{\sqrt{6}}(\mathbf{x}_1' + \mathbf{x}_2' - 2\mathbf{x}_3') \quad \mathbf{p}_\lambda = \frac{1}{\sqrt{6}}(\mathbf{p}_1' + \mathbf{p}_2' - 2\mathbf{p}_3'). \tag{5}$$

W.B. Zhao et al, Phys.Lett.B 820 (2021) 136571

Compound Yield Ratio

$$\frac{N_t \times N_p}{N_d^2} \approx \frac{1}{2\sqrt{3}}\left[1 + \Delta n + \frac{\lambda}{\sigma} G\left(\frac{\xi}{\sigma}\right)\right]$$

- λ is a parameter that varies smoothly with T and μ_B of emission source
- $\sigma \approx r_d \approx r_t$ is the root-mean-radius of light nuclei

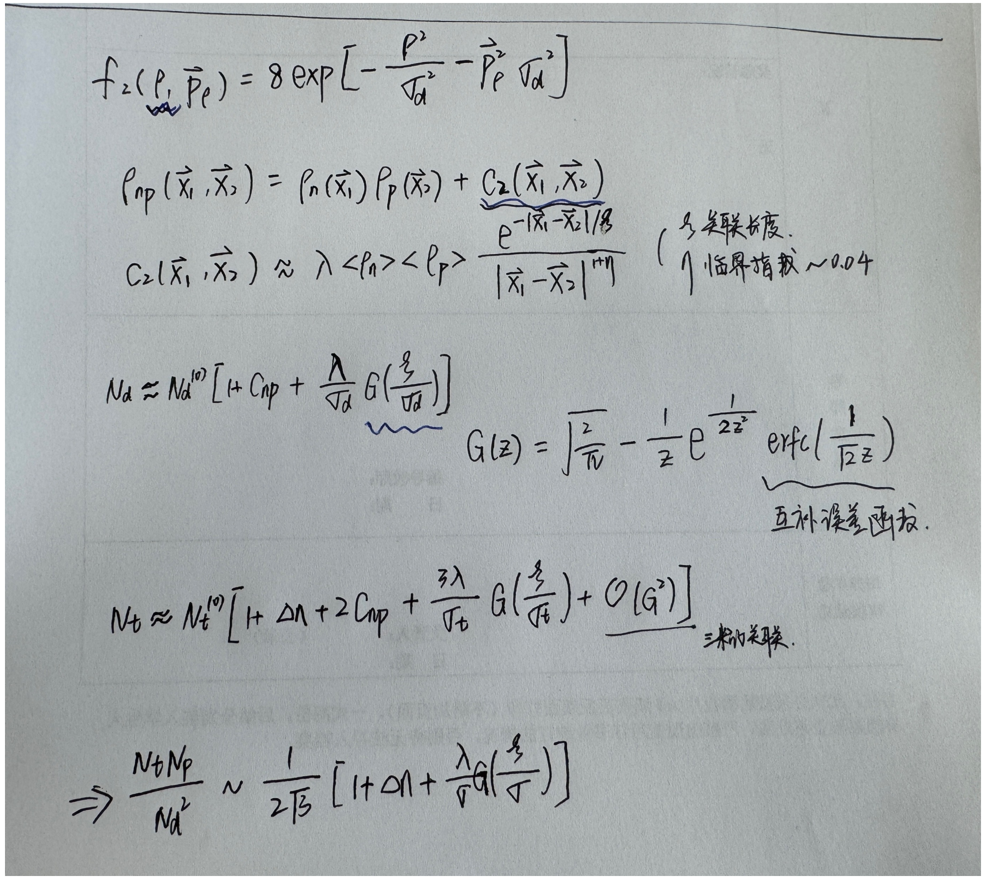

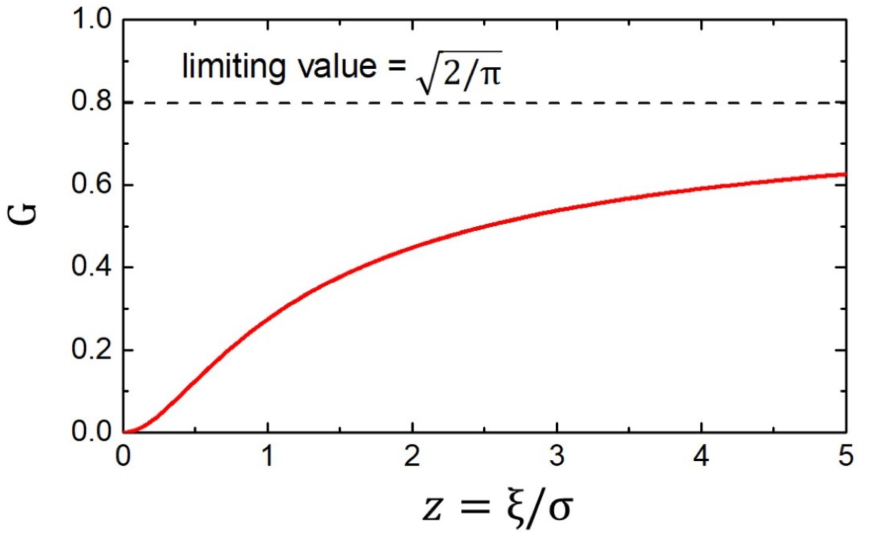

FIG. 1: The dependence of the function $G(\xi/\sigma)$ on the correlation length ξ with σ being the width parameter in the deuteron or triton Wigner function.

V. Koch, arXiv:0810.2520;
J. Zinn-Justin, Phys.Rept. 344 (2001) 159-178;
K.J. Sun et al, Phys.Lett.B 816 (2021) 136258